

The samples were prepared in such a way that the same substrate carried thick- and thin-film junctions (the configuration of the samples is shown in Fig. 3a). This enabled us to obtain, in the same experiment, additional information on the isotropic energy gap $2\Delta_{AV}$. This method eliminated the error in the determination of the pressure when the results for the isotropic and anisotropic components of the gap were compared. At all pressures, we found that $\Delta_{AV} = (\Delta_1 + \Delta_2)/2$. The pressure-induced change in the energy gap of thin films was in agreement with our earlier results.^[4]

The features at $eU > \Delta_{Al} + \Delta_{Pb}$, associated with the phonon spectrum of the superconductor, were investigated using thin-film ($\sim 1000 \text{ \AA}$) superconducting junctions. An investigation of the S-I-S system enabled us to resolve (and obtain information on) three peaks in the phonon spectrum obtained for the transverse polarization under pressure (Fig. 5). Table I gives the results of the present investigation, as well

as the results obtained by others.^[5,6,30] It is evident from Table I that, basically, the various tunnel-effect data are in good agreement.

The main results of the theory of anomalous superconductors due to Geilikman and Kresin^[31]

$$\frac{2\Delta}{kT_c} = 3.52 \left[1 + 5.3 \frac{T_c^2}{\omega_0^2} \ln \frac{\omega_0}{T_c} \right], \quad (2)$$

and of the theory due to McMillan^[32]

$$T_c = \frac{\omega_c}{1.73} \exp \left[-\frac{1.04(1+\lambda)}{\lambda - \mu^*(1+0.62\lambda)} \right] \quad (3)$$

can be applied to the experimental results.^[6] For convenience, we can rewrite Eqs. (2) and (3) in the differential form:^[33]

$$\frac{d \ln T_c}{dP} = \left[\frac{d \ln 2\Delta}{dP} + 5.3 \frac{d \ln \omega_0}{dP} \cdot \left(2 \ln \frac{\omega_0}{T_c} - 1 \right) \frac{T_c^2}{\omega_0^2} \right] \left[1 + 5.3 \frac{T_c^2}{\omega_0^2} \times \left(2 \ln \frac{\omega_0}{T_c} - 1 \right) \right]^{-1}, \quad (4)$$

$$\frac{d \ln T_c}{dP} = \frac{d \ln \omega_c}{dP} + \frac{1.23}{(\lambda - 0.11)^2} \cdot \sum_{\nu} \lambda_{\nu} \left(\frac{d \ln I_{\nu}}{dP} - 2 \frac{d \ln \omega_{\nu}}{dP} \right). \quad (5)$$

Here, ω_0 is the characteristic frequency of phonons (ω_t or ω_l); ω_c is the cutoff frequency; λ is the elec-

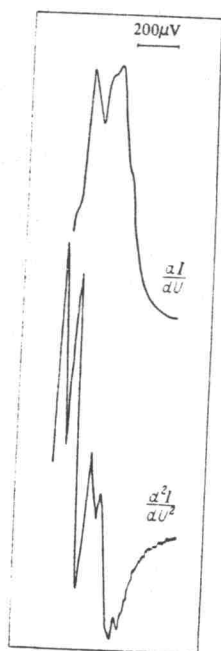


FIG. 2. Complex structure of the $(dI/dU) = f(U)$ and $(d^2I/dU^2) = F(U)$ characteristics of an Al-I-Pb* sample in the vicinity of the sum of the energy gaps $\Delta_{Pb} + \Delta_{Al}$, $T = 1.16^\circ\text{K}$.

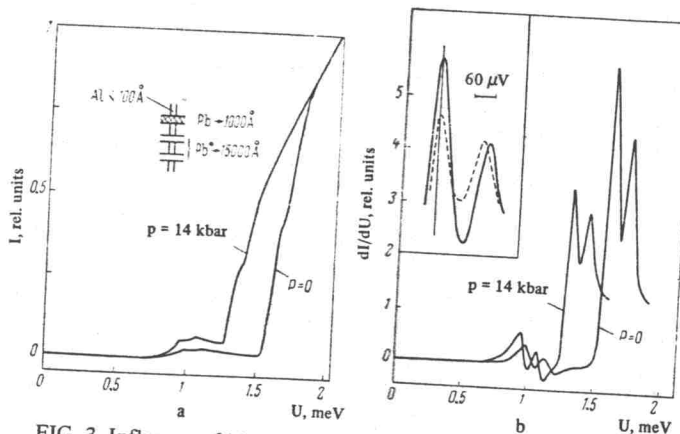


FIG. 3. Influence of high pressures on the characteristics of an Al-I-Pb* sample: a) $I = f(U)$; b) $(dI/dU) = F(U)$, $T = 1.17^\circ\text{K}$. The insert shows the pressure-induced shift $\Delta_{Pb}^p - \Delta_{Pb}^0$ (the dashed curve corresponds to a pressure of 14 kbar).

Table I. Results of investigations of the tunnel effect in lead under pressure

	Investigated quantity X			
	$2\Delta_1$	$2\Delta_{cp}$	$2\Delta_2$	
X, meV	2.56 ± 0.01	2.72 ± 0.01 2.71 [8]	2.85 ± 0.01	
dX/dP , 10^{-5} meV/bar	-2.22 ± 0.15	-2.34 ± 0.15 -2.16 ± 0.2 [8]	-2.45 ± 0.15	
$d \ln X/dP$, 10^{-6} bar $^{-1}$	-8.7 ± 0.6	-8.6 ± 0.6 -10.1 ± 0.8 [8] -8 [8]	-8.6 ± 0.6	
	Investigated quantity X			
	ω_t^+	ω_t^-	ω_l^-	ω_l^+
X, meV	3.88 ± 0.02	4.52 ± 0.02 4.45 [8] 4.6 [30]	4.9 ± 0.02	8.55 ± 0.02 8.5 [8]
dX/dP , 10^{-5} meV/bar	2.6 ± 0.4	3.3 ± 0.4 4.5 ± 0.6 [8]	3.3 ± 0.4	6.4 ± 0.4 6 ± 0.6 [8]
$d \ln X/dP$, 10^{-6} bar $^{-1}$	6.75 ± 1	7.28 ± 1 5.3 ± 0.7 [30] 10.1 [8]	6.75 ± 1	7.5 ± 0.5 7 ± 0.7 [30] 7.05 [8]